

GSA Data Repository Item 2018096

Nicholas J.R. Hunter, Roberto F. Weinberg, Christopher J.L. Wilson, Vladimir Luzin, Santanu Misra, 2018, Microscopic anatomy of a “hot-on-cold” shear zone: Insights from quartzites of the Main Central Thrust in the Alaknanda region (Garhwal Himalaya): Geological Society of America Bulletin, v. 130, no. 9-10, p. 1519–1539, <https://doi.org/10.1130/B31797.1>.

DATA REPOSITORY

Figures S1–S3, Table S1.

Pole figure intensity calculations and MTEX scripts for analyzing quartz pole figures.

demo_001.txt

demo_100.txt

demo_101.txt

demo_110.txt

Intensity_spectrum_analysis.m

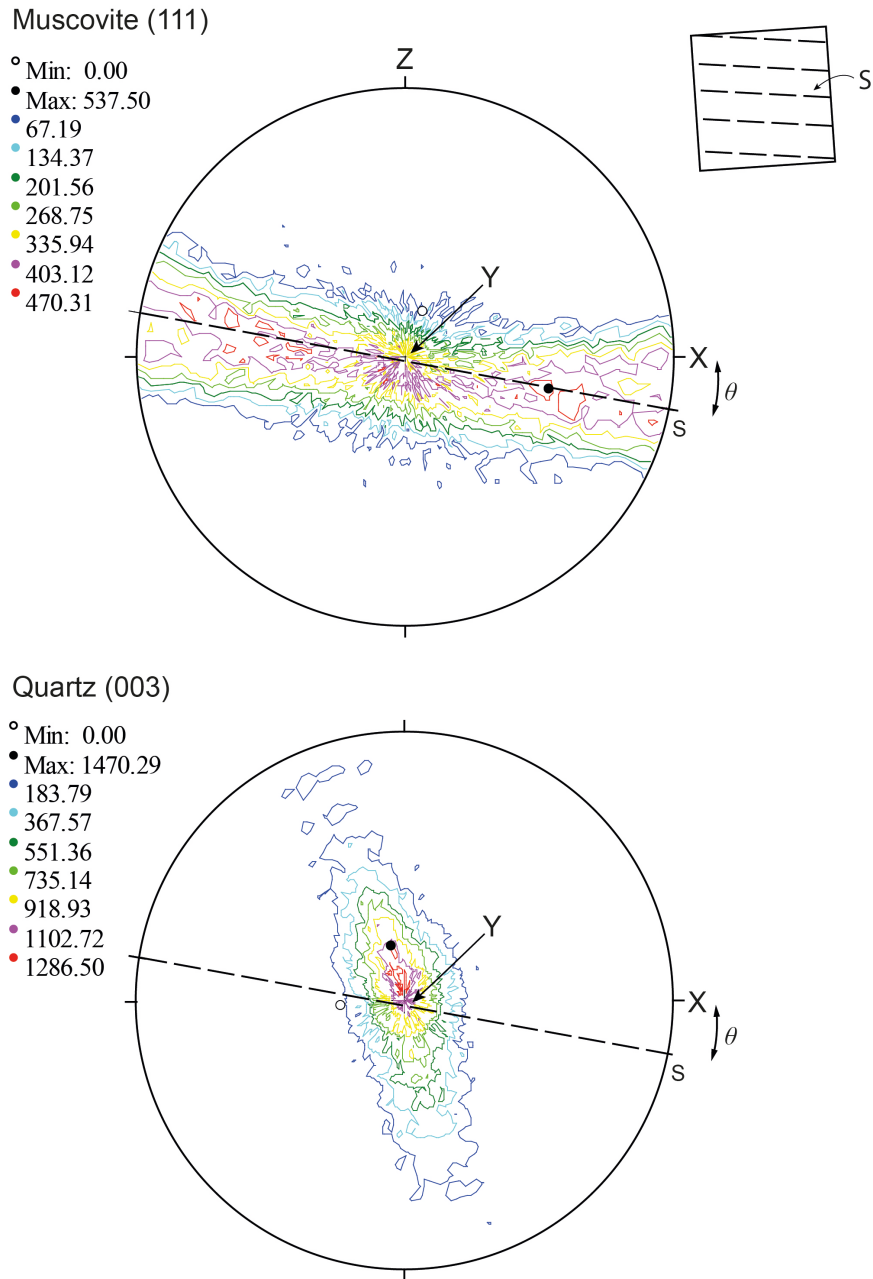


Figure S1 – Method for reorienting pole figures using mica (110)+(111) pole figures. In some instances, sample cubes may be irregularly cut, or positioned at a slight angle to the incident neutron beam, which causes the tectonic foliation (S) to be slightly offset from horizontal (top right). Sample offsets of this type may be corrected by using a mica (110)+(111) pole figure from the same cube specimen, which expresses S as a horizontal girdle. Thus the (110)+(111) muscovite pole figure, and all other pole figures in the specimen, can be rotated about Y back into parallelism with the east-west kinematic reference plane X over an angle ϑ .

Figure S2 - Routine for calculating 'intensity spectrum' for *c* and *a* pole figures in MTEX. An accompanying MATLAB script and demo pole figure files have been provided.

```
%% Calculate intensity spectrum for c-axis pole figures
% Version 1.1
%
% This script constructs the intensity spectrum in c-axis ODF pole figures
% at 5 degrees plunge. This routine allows the user to identify peaks
% associated with orthorhombic and monoclinic c-axis symmetries and thus
% semi-quantify coaxial and non-coaxial deformations, kinematics, vorticity
% and opening angle geometries.
%
% Requires MATLAB R2012B or higher, and MTEX 4.0 or higher

clear all
%% Specify Crystal and Specimen Symmetries

% crystal symmetry
CS = crystalSymmetry('-3m', [4.916 4.916 5.4054], 'mineral', 'Quartz',
'color', 'light blue');

% specimen symmetry
SS = specimenSymmetry('1');

% plotting convention
setMTEXpref('xAxisDirection','east');
setMTEXpref('zAxisDirection','outOfPlane');
%% Specify File Names
% NOTE: the file path will need to be changed based on the location of the
% demo files! Please modify in scriptline 29

% path to files
pname = 'G:\MCT\Models';

% which files to be imported
fname = {...
    [pname '\demo_001.txt'],...
    [pname '\demo_100.txt'],...
    [pname '\demo_101.txt'],...
    [pname '\demo_110.txt'],...
};
%% Specify Miller Indices

h = { ...
    Miller(0,0,1,CS),...
    Miller(1,0,0,CS),...
    Miller(1,0,1,CS),...
    Miller(1,1,0,CS),...
};
%% Import the measured data
% create a Pole Figure variable containing the data
pf = loadPoleFigure(fname,h,CS,SS,'interface','generic',...
    'ColumnNames', { 'Latitude' 'Longitude' 'Intensity'});
%% Plot pole figures for visual inspection
plot(pf,'lower', 'contourf', 'contours', 13)
%% Create an ODF from measured data to complete texture
odf_quartz = calcODF(pf,'halfwidth',5*degree)
```

```

%% Set Miller Indices
pfs_qtz_hkl = (...
    [Miller(0,0,0,3,CS, 'Quartz', 'hkl')...
    Miller(1,1,-2,0,CS, 'Quartz', 'hkl'),...
    ])
% list two : [uvw] [directions]
pfs_qtz_uvw = (...
    [Miller(0,0,0,3,CS, 'Quartz', 'uvw')...
    Miller(1,1,-2,0,CS, 'Quartz', 'uvw'),...
    ])
%% Plot 001 and 110 pole figures for inspection of ODF routine
figure
plotPDF(odf_quartz,pfs_qtz_hkl, 'lower')
%% Calculate the intensity spectrum along 001 for theta = 5 degrees
% Note that azimuth = 0 starts at 90 and rotates counter-clockwise.
r = vector3d('rho', (0:360)*degree, 'theta', 5);
intensity_raw = calcPDF(odf_quartz,Miller(0,0,1,odf_quartz.CS),r);
% Convert counter-clockwise to clockwise
intensity_rotate = flipud(intensity_raw);
% Modify data set to start at Y (0 degrees) in pole figure
intensity = circshift(intensity_rotate,90);
% Plot the figure
figure
plot(r.rho./degree,intensity)
set(gca, 'xtick', [-180 -150 -120 -90 -60 -30 0 30 60 90 120 150 180])
set(gca, 'xtickLabel',
{'0', '30', '60', '90', '120', '150', '180', '210', '240', '270', '300', '330', '360'})
xlabel('Azimuth of pole figure')
ylabel('Intensity')
% Return values for peaks (intensity, azimuth)
[pks_001, az_001] = findpeaks(intensity)
%% Calculate angle between highest density c-axis maxima and foliation normal
(Z)
%
% Used to assist in determining flow vorticity (Willis et al 1995).
% -x = sinistral
% +x = dextral
%
% Top maxima
[c_max_t,id_max_001_t] = max(intensity)
c_max_angle_t = minus(90,id_max_001_t)
%% Calculate opening angles for c-axis pole figure
%
% If an orthorhombic symmetry is detected, the opening angle can be
% measured between crossing girdles.
%
% Detect four highest values associated with girdles
n = numel(pks_001);
id = [1:n]';
angle = [pks_001, az_001 id];
az_max = sortrows(angle, -1);
id_four = az_max(1:4, [2 3]);
id_four_sort = sortrows(id_four, 2);
% Take difference between north and south girdles and return the mean
oa_correct = minus(360, id_four_sort(4));
oa_top = plus(oa_correct,id_four_sort(1))
oa_bottom = minus(id_four_sort(3),id_four_sort(2))
mean_oa = (oa_top+oa_bottom)/2

```

Figure S3: Measurements of CPO intensity

To analyse CPO intensity, we have employed several types of measurement that can broadly be classified into two groups. The first group we have defined as ‘ODF-based measurements’, which calculate the proximity of the total texture in Euler space. The most common of these is the J -index, first applied to metals by Sturcken and Croach (1963), which measures the squared integral difference between an observed ODF and a uniform (i.e. random) distribution function. While the method offers a more ‘complete’ estimation of the bulk texture intensity, several shortcomings of the technique have been raised (Skemer et al., 2005; Wenk and Van Houtte, 2004; Xie et al., 2003). An alternative measurement is the texture entropy (TE) of Schaeben (1988). Both J and TE are calculated directly from the ODF, and the resulting values are therefore dependent on the crystal symmetry, specimen symmetry, kernel density and half-width.

The second group we have defined as ‘eigenvalue-based measurements’, which are derived from the normalized eigenvalues in the orientation tensor of a single pole figure (Scheidegger, 1965; Watson, 1966). Eigenvalues λ_1 , λ_2 , and λ_3 describe the variance associated with the eigenvectors defining the orientation tensor, and are typically normalized (S) so that $S_1 + S_2 + S_3 = 1$. The relationship between these values is characteristic of certain clustering shapes: (i) ‘point’ or ‘cluster’ distribution are defined by $S_1 > S_2 \approx S_3$; (ii) ‘girdle’ or ‘planar’ distributions are defined by $S_1 \approx S_2 > S_3$; and (iii) ‘random’ or ‘isotropic’ distributions are defined by $S_1 \approx S_2 \approx S_3$. The relationships between these eigenvalues can be used to compute two quantitative estimates of intensity of the axial data. Eigenvalue-based intensity analysis are particularly useful, as values are generally independent of sample size, and the measurements are easy to calculate (Woodcock, 1977; Woodcock and Naylor, 1983). Most importantly, eigenvalue-based calculations are not restricted to ODF, and thus calculations can be made using data across the broader suite of textural analysis instruments, including the universal stage and automated fabric analysers. However, previous workers have discussed the shortcomings of eigenvalue-based parameters for crystallographic texture analysis for resolving axial distributions with orthorhombic symmetry such as crossed girdle maxima (Mainprice et al., 2015; Starkey, 1993).

For our analysis of CPO intensity, we have modified the uniformity test statistic of Mardia (1972), which was originally expressed as:

$$U = \frac{15n}{2} \sum_{i=1}^3 \left(S_i - \frac{1}{3}n \right)^2$$

Where S_i describes the normalised eigenvalue. Here, if U exceeds the critical values for a null distribution, where $S_1 = S_2 = S_3 = 1/3$, it can be said to deviate from uniformity and therefore

contains a non-uniform distribution, where higher U values indicate higher intensity. The null hypothesis of uniformity is rejected with 95% and 99% confidence where U exceeds values of 11.07 and 15.09, respectively (Lisle, 1985; Mardia, 1972). This statistic was modified for geological purposes by Lisle (1985) to a sample size insensitive form:

$$I = \frac{15}{2} \sum_{i=1}^3 \left(S_i - \frac{1}{3} \right)^2$$

However, in both former calculations it is unlikely that such a highly isotropic distribution, where all eigenvalues equal $1/3$, will be found in nature, and thus approximating 'randomness' in rocks can be limited using this statistic. We thus modify the equation so that I becomes the measure of deviation between the eigenvalues of a deformed sample (S_{iD}) and an undeformed protolith (S_{iP}). In this scenario, the uniformity statistic simply becomes:

$$I_P = \frac{15}{2} \sum_{i=1}^3 (S_{iD} - S_{iP})^2$$

This approach has several improvements on previous calculations: (i) texture strength is directly related to the undeformed host rock, and thus is similar to classic strain analysis tests (Lisle, 1977); (ii) any previous deformation textures recorded in the protolith are taken into account during the test. We have used an undeformed rock from the MCT sequence (AK-76) as a protolith.

In summary, we have used four calculations for bulk texture intensity analysis in our paper: (i) the J -index; (ii) the texture entropy (TE); (iii) the original n -insensitive intensity parameter of Lisle (1985) (I); and (iv) the modified form of I , where intensity is related to the protolith (I_P).

REFERENCES

- Lisle, R. J., 1977, Estimation of the tectonic strain ratio from the mean shape of deformed elliptical markers: *Geologie en Mijnbouw*, v. 56, no. 2, p. 140-144.
- Lisle, R. J., 1985, The use of the orientation tensor for the description and statistical testing of fabrics: *Journal of Structural Geology*, v. 7, no. 1, p. 115-117.
- Mainprice, D., Bachmann, F., Hielscher, R., and Schaeben, H., 2015, Descriptive tools for the analysis of texture projects with large datasets using MTEX: strength, symmetry and components: *Geological Society, London, Special Publications*, v. 409, no. 1, p. 251-271.
- Mardia, K. V., 1972, *Statistics of Directional Data*, London, Academic Press.
- Schaeben, H., 1988, Entropy optimization in quantitative texture analysis: *Journal of Applied Physics*, v. 64, no. 4, p. 2236-2237.
- Scheidegger, A. E., 1965, On the statistics of the orientation of bedding planes, grain axes, and similar sedimentological data, U.S. Geologic Survey Professional Paper.

- Skemer, P., Katayama, I., Jiang, Z., and Karato, S. I., 2005, The misorientation index: Development of a new method for calculating the strength of lattice-preferred orientation: *Tectonophysics*, v. 411, no. 1-4, p. 157-167.
- Starkey, J., 1993, The analysis of three-dimensional orientation data: *Canadian Journal of Earth Sciences*, v. 30, no. 7, p. 1355-1362.
- Sturcken, E. F., and Croach, J. W., 1963, Predicting physical properties in oriented metals: *Transactions of the Metallurgical Society of AIME*, v. 227, p. 934-940.
- Watson, G. S., 1966, The statistics of orientation data: *The Journal of Geology*, v. 74, no. 5, p. 786-797.
- Wenk, H. R., and Van Houtte, P., 2004, Texture and anisotropy: *Reports on Progress in Physics*, v. 67, no. 8, p. 1367-1428.
- Woodcock, N. H., 1977, Specification of fabric shapes using an eigenvalue method: *Geological Society of America Bulletin*, v. 88, no. 9, p. 1231-1236.
- Woodcock, N. H., and Naylor, M. A., 1983, Randomness testing in three-dimensional orientation data: *Journal of Structural Geology*, v. 5, no. 5, p. 539-548.
- Xie, Y., Wenk, H.-R., and Matthies, S., 2003, Plagioclase preferred orientation by TOF neutron diffraction and SEM-EBSD: *Tectonophysics*, v. 370, no. 1-4, p. 269-286.

TABLE S1. Raw and normalised intensities of quartz pole figures

	<i>Texture intensities</i>				<i>Normalised texture intensities</i>			
	I_P^a	I_R^b	J-index	Texture entropy	I_P^a	I_R^b	J-index	Texture entropy
AK-76	0.00	0.16	1.23	-0.10	0.00	0.02	0.04	0.02
AK-43	0.25	0.63	2.59	-0.52	0.07	0.08	0.09	0.10
AK-2	0.38	0.64	2.05	-0.42	0.11	0.08	0.07	0.08
AK-2 EBSD	0.34	0.63	-	-	0.10	0.08		
AK-44	0.20	0.40	1.69	-0.29	0.06	0.05	0.06	0.06
AK-45	0.49	0.86	2.85	-0.60	0.14	0.11	0.10	0.12
AK-6-1	0.81	1.66	5.35	-0.86	0.23	0.22	0.20	0.17
AK-6 EBSD	0.86	1.72	-	-	0.24	0.23		
AK-84-6	0.47	0.98	3.53	-0.74	0.13	0.13	0.13	0.15
AK-86	0.50	1.18	4.24	-0.81	0.14	0.16	0.15	0.16
AK-91 EBSD	0.46	1.14	-	-	0.13	0.15		
AK-95-3	0.37	0.96	2.93	-0.63	0.10	0.13	0.11	0.13
AK-90	0.06	0.05	1.15	-0.07	0.01	0.00	0.04	0.01

Note: J-index and texture entropy values are sensitive to the different measurement conditions between EBSD and neutron diffraction and are thus not comparable. As a result, values are not calculated for EBSD data.

^a Modified intensity factor of Lisle [1985], refer Appendix

^b Intensity factor of Lisle [1985]